MATCH
Communications in Mathematical and in Computer Chemistry

MATCH Commun. Math. Comput. Chem. **96** (2026) 129–157
ISSN: 0340–6253
doi: 10.46793/match.96-1.28125

Fractional Modeling of Cooperative Enzyme Kinetics with Neural Network Validation

Rana Muhammad Zulqarnain[a], Israr Ahmad[b], Gauhar Ali[b], Rifaqat Ali[c], Yong Wang[d,*], Muhammad Marwan[d,*]

[a] *School of Business, Xian International University, Xian, Shaanxi, China*

[b] *Department of Mathematics, Government Post Graduate Jahanzeb College, Swat, Khyber Pakhtunkhwa, Pakistan*

[c] *Department of Mathematics, Applied College in Mohayil Asir, King Khalid University, Abha, Saudi Arabia*

[d] *School of Mathematics and Statistics, Linyi University, Linyi, Shandong, China*

ranazulqarnain@zjnu.edu.cn, israrahmad@jc.edu.pk, gauharali@gmail.com, rrafat@kku.edu.sa, wangyongf2@lyu.edu.cn, marwan78642@zjnu.edu.cn

(Received October 27, 2025)

Abstract

In this study, we develop a fractional-order cooperative enzymatic reaction model using the Liouville–Caputo derivative to extend its kinetics. We present the existence and uniqueness of the solutions through the theory of nonlinear functional analysis. We find the numerical solutions of the specified model using the Euler method and the Laplace Adomian decomposition method (LADM). The precision of the considered technique is evaluated with the

*Muhammad Marwan and Yong Wang are corresponding authors

aid of Levenberg-Marquardt neural network (NN) platform, complemented with regression analysis and error distribution statistics. The data are divided into several sets including training (70%), validation (15%), and testing (15%). The approximate solutions are analyzed graphically using $2D$ and $3D$ phase portraits for various fractional orders and reaction parameters with the help of MATLAB R2024a. Furthermore, a comparative analysis of numerical solutions is presented for both integer and fractional order dynamical systems. This approach provides a new way to chemical reactions and presents the dynamics of these reactions in a new look under fractional derivatives. These findings highlight the potential of fractional calculus (FC) as a powerful modeling framework for complex biochemical kinetics. The framework introduced here provides a theoretical foundation that may support future research in optimizing biochemical processes, including applications in metabolic engineering and controlled drug release mechanisms.

Introduction

Enzymatic reactions are extremely essential to most biochemical processes since they govern physiological process and metabolic pathways in living organisms, [13, 33, 38]. Mathematical modeling of such reactions helps in studying reaction efficiencies, substrate dynamics, and enzyme kinetics [21]. Generally, biochemical reactions are usually discussed with classical differential equations of integer order. Amen investigated the dynamics of a small autonomous three-dimensional biochemical reaction system [6]. A lorenz-based chemical reaction system is studied by Marwan et. al [30] for seeking fractals in their trajectories. In 2024, Kreikemeyer et al. [24] worked on enzyme chemical reaction model by extracting its data using sparse identification method to elaborate its nonlinear dynamics. Sometimes, such models are unable to accommodate effects of long-range dependencies and memory effect, which characterize complex biological systems. In order to overcome such limitations, generalized frameworks like fractional calculus must be taken into account.

Fractional calculus provides more generalized form as compared to classical calculus and gives more fluctuation. Fractional order systems have potential applications in pharmaceutical research, metabolic engineering, and optimization of biochemical processes [3, 7, 31]. This provides more appro-

priate framework that describes non-local interactions and unique hereditary properties present in biochemical and other systems [11,14,26,35,36]. Over the past ten years, fractional order models have attracted much attention in the modeling of anomalous diffusion, memories over long periods of time, and fractal-like behavior in different scientific activities such as biology [25], physics [1,5], and engineering, [15]. Therefore, it is evident that fractional-order models attract attention due to their ability to describe biochemical reactions while facing failure in integer-order models.

Recent studies have indicated that within a set of long-range dependencies and diffusion effects, enzyme reactions show a complex kinetic behavior [10]. Classical Michaelis-Menten kinetics [29], relying on an integer-order model, assumes local and instantaneous interactions between enzymes and substrates. Though biochemical reactions often involve time-dependent memory effects that cannot be captured satisfactorily through classical descriptions [22]. An alternative enzymatic reaction model that permits a fractional differential approach amended this inconvenience and allows extra flexibility in depicting the reaction dynamics.

Chemical reactions and mathematics are interconnected through giving shape of differential equations to to the balancing of chemical reactions. In 2025 Gao et al. [16] discussed the codimension-one and codimension-two bifurcations of an auto-catalyst chemical reactions-based system. A reaction-diffusion model of glucose and chemical retrial queue models are being studied by Izadi et al. [19] and Mathavavisakan et al. [27], respectively. The large chemical reaction network for the atom transition and isotope labeling patterns is discussed by Golnik et al. [17]. There are more dynamical systems designed on the basis of chemical reactions in the literature, but the following system (1) that we considered in our current study is based on the following kinetic scheme that extends the classical Michaelis-Menten mechanism:

$$\begin{aligned} \mathrm{S} + \mathrm{E} &\underset{\beta}{\overset{\alpha}{\rightleftharpoons}} \mathrm{C} \xrightarrow{\gamma} \mathrm{P} + \mathrm{E}, \\ \mathrm{S} + \mathrm{C} &\underset{\eta}{\overset{\omega}{\rightleftharpoons}} \mathrm{Q} \xrightarrow{\sigma} \mathrm{P} + \mathrm{C}, \end{aligned}$$

where $S(t)$ represents the concentration of substrate, $C(t)$ shows the con-

centration of a single bound substrate-enzyme complex, $Q(t)$ is the concentration of dual bound substrate-enzyme complex, $E(t)$ is the concentration of enzyme, $P(t)$ presents the concentration of product.

The enzyme $E(t)$ binds a substrate $S(t)$ to form a single bound substrate-enzyme complex enzyme $C(t)$. This complex enzyme $C(t)$ not only breaks down to form a product $P(t)$ and the enzyme $E(t)$ again, but it can also combine with another substrate molecule to form a dual-bound substrate-enzyme complex $Q(t)$. This $Q(t)$ breaks down to form product $P(t)$ and the single bound $C(t)$. The parameters α and β are the forward and reverse rate constants for the primary binding step. The parameter γ is the catalytic rate constant for $C(t)$. The parameter ω governs the rate of second substrate binding. The parameters η and σ are the dissociation and catalytic rate constants for the dual-bound $Q(t)$.
After applying the law of mass action to the above kinetic scheme, we have the following system of differential equations [32, Sec. 5.3, p. 119]:

$$\begin{cases} \dfrac{dS(t)}{dt} = -\alpha S(t)E(t) + \beta C(t) - \omega S(t)C(t) + \eta Q(t), \\ \dfrac{dC(t)}{dt} = \alpha S(t)E(t) - (\beta+\gamma)C(t) - \omega S(t)C(t) + (\eta+\sigma)Q(t), \\ \dfrac{dQ(t)}{dt} = \omega S(t)C(t) - (\eta+\sigma)Q(t), \\ \dfrac{dE(t)}{dt} = -\alpha S(t)E(t) + (\beta+\gamma)C(t), \\ \dfrac{dP(t)}{dt} = \gamma C(t) + \sigma Q(t), \end{cases} \tag{1}$$

with the initial conditions $S(0) = S^0$, $C(0) = C^0$, $Q(0) = Q^0$, $E(0) = E^0$, $P(0) = P^0$. The conservation of the enzyme is obtained by summing the second, third and fourth equations of the system (1), it is straightforward to verify that $\frac{d}{dt}\left[E(t) + C(t) + Q(t)\right] = 0$ and using the initial conditions; it is $E(t) + C(t) + Q(t) = E_0$.

Fractional order models can be applied to multi-enzyme systems [39], allosteric regulation [18], and cooperative enzymatic behavior [20] with multiple interacting species. The flexibility of FC in capturing non-local effects makes it an ideal framework for exploring biochemical reactions

that exhibit time-dependent and spatially heterogeneous properties such as drug formulations [4], enzyme-based biosensors [40], and metabolic pathway simulations [28]. In this work, the classical cooperative enzymatic reaction model is extended to the Liouville–Caputo fractional-order model

$$\begin{cases} {}^{LC}D^{\theta}_{0,t}S(t) = -\alpha S(t)E(t) + \beta C(t) - \omega S(t)C(t) + \eta Q(t), \\ {}^{LC}D^{\theta}_{0,t}C(t) = \alpha S(t)E(t) - (\beta+\gamma)C(t) - \omega S(t)C(t) + (\eta+\sigma)Q(t), \\ {}^{LC}D^{\theta}_{0,t}Q(t) = \omega S(t)C(t) - (\eta+\sigma)Q(t), \\ {}^{LC}D^{\theta}_{0,t}E(t) = -\alpha S(t)E(t) + (\beta+\gamma)C(t), \\ {}^{LC}D^{\theta}_{0,t}P(t) = \gamma C(t) + \sigma Q(t), \end{cases} \tag{2}$$

with the initial conditions $S(0) = S^0, C(0) = C^0, Q(0) = Q^0, E(0) = E^0, P(0) = P^0$. The system (2) is the extension or generalization of the system (1); we can get the model (1) by putting $\theta = 1$. This specific derivative is one of those most relevant when modeling physical and biological systems [9]. Therefore, this analysis helps in better determining dynamics of reaction models such as substrate concentration, enzyme concentration, and product concentration at a given time. In this case, fractional differentiation achieves the objective of improving the prediction power of an enzymatic model and allowing the creation of models that can accurately reflect enzyme kinetics.

Apart from this, to find the mathematical soundness of the specified model, existence and uniqueness of solutions is one of the best tool, using nonlinear functional analysis, to investigate further dynamics. This theoretical framework guarantees that the model is well-posed and delivers meaningful solutions under the prescribed initial conditions. Additionally, the LADM and Euler method [2] are used to obtain the approximate solutions, ensuring computational efficiency and accuracy. Recently, Bilal et al. [8] utilized artificial neural networks in irreversible biochemical reactions but the dynamics of fractional-order enzyme reaction system in artificial neural networks still need to be discussed.

In this paper we have worked on the following points to cover several problems including:

(1) Complete study of enzyme reaction dynamics under varying fractional orders and parameters of the reaction.

(2) Numerical solutions are achieved and compared for both integer and fractional order systems.

(3) The influence of fractional calculus is examined on the kinetics our proposed dynamical system.

(4) How the stability and efficiency of enzymatic reactions are affected by various fractional order is integral part of the current work.

The importance of our study is not limited to theoretical contributions but has variety of applications in neural networking as well. Moreover, this work provides a guidance for future work on enzyme-substrate interactions, catalysis, and large study sets of biochemical networks by showing that FC can be applied to modeling enzymatic reactions.

The subsequent sections are structured as follows. In Section 1, fundamental definitions, lemmas and theorems are given to understand analytical results in the paper with ease. Qualitative analysis of the transformed dynamical system is discussed in Section 2. Numerical simulations of the analytical results provided in previous sections are plotted and discussed in Section 3, while the concluding remarks are given in the Section 4.

1 Preliminaries

The present section consist of fundamental definitions, Lemma and theorem that are considered as useful tools in rest of the paper. We created a Banach space $(\mathbb{W}, ||.||)$, with norm $\|z\| = \underset{t\in J}{max}\big|z(t)\big|$, where $t \in [0, \varpi] = J$. Consequently, we get $\mathbf{W} = \mathbb{W}^5$ a Banach space with norm $||(S, C, Q, E, P)|| = \underset{t\in J}{max}\{||S||, ||C||, ||Q||, ||E||, ||P||\}$ for system (2).

Definition 1. [23] Suppose that $\theta \in (0, 1)$, then the fractional integral for a function $z(t)$ is

$$I^{\theta}_{0,t} z(t) = \frac{1}{\Gamma(\theta)} \int_0^t (t-\kappa)^{\theta-1} z(\kappa) d\kappa. \tag{3}$$

Definition 2. [23] Let $\theta \in (0,1)$, then for a function $z(t)$ the fractional Liouville–Caputo derivative is

$$^{LC}D^{\theta}_{0,t}z(t) = \frac{1}{\Gamma(1-\theta)}\int_0^t (t-\kappa)^{-\theta} z'(\kappa)d\kappa, \tag{4}$$

where $z(t)$ is absolutely continuous on the interval $[0,t]$, and ensures the existence of the ordinary derivative $z'(\kappa)$ almost everywhere.

Definition 3. The Laplace transformation for the Liouville–Caputo derivative (4) gives

$$\mathbb{L}[^{LC}D^{\theta}_{0,t}z(t)] = s^{\theta}Z(s) - s^{\theta-1}z(0), \tag{5}$$

where $Z(s)$ is the Laplace transformation of $z(t)$.

Lemma 1. *The solution of the fractional differential equation* $^{LC}D^{\theta}_{0,t}z(t) = g(t)$ *with the initial condition* $z(0) = z^0$*, using Riemann–Liouville fractional integral* (3)*, can be written as*

$$z(t) = z^0 + \frac{1}{\Gamma(\theta)}\int_0^t (t-\kappa)^{\theta-1} g(\kappa)d\kappa.$$

Theorem 1. *[12, 41] Let* $\mathbb{B}$ *be a convex, closed, and bounded subset of a Banach space* $\boldsymbol{W}$*, and let* $\mathbb{T} : \mathbb{B} \to \mathbb{B}$ *be a continuous and compact operator, then* $\mathbb{T}$ *has at least one fixed point in* $\mathbb{B}$*.*

2 Qualitative study of the specified model

In this section, we investigated qualitative analysis of the solutions achieved using the theory of nonlinear functional analysis. In Theorem 2, we presented the uniqueness of a solution for the fractional-ordered dynamical system (2), and in Theorem 3 the existence of its solutions is discussed.

In rest of the paper, we rewrite system (2) in the following form

$$\begin{cases} {}^{LC}D^{\theta}_{0,t}S(t) = \Phi_1(S,C,Q,E,P), \\ {}^{LC}D^{\theta}_{0,t}C(t) = \Phi_2(S,C,Q,E,P), \\ {}^{LC}D^{\theta}_{0,t}Q(t) = \Phi_3(S,C,Q,E,P), \\ {}^{LC}D^{\theta}_{0,t}E(t) = \Phi_4(S,C,Q,E,P), \\ {}^{LC}D^{\theta}_{0,t}P(t) = \Phi_5(S,C,Q,E,P), \end{cases}$$

where

$$\begin{cases} \Phi_1(S,C,Q,E,P) = -\alpha S(t)E(t) + \beta C(t) - \omega S(t)C(t) + \eta Q(t), \\ \Phi_2(S,C,Q,E,P) = \alpha S(t)E(t) - (\beta+\gamma)C(t) - \omega S(t)C(t) + (\eta+\sigma)Q(t), \\ \Phi_3(S,C,Q,E,P) = \omega S(t)C(t) - (\eta+\sigma)Q(t), \\ \Phi_4(S,C,Q,E,P) = -\alpha S(t)E(t) + (\beta+\gamma)C(t), \\ \Phi_5(S,C,Q,E,P) = \gamma C(t) + \sigma Q(t). \end{cases} \tag{6}$$

Furthermore, the class of fractional order systems can be rewritten in the following compact form:

$$\begin{cases} {}^{LC}D^{\theta}_{0,t}F(t) = G(t,F(t)), \\ F(0) = F^0, \end{cases} \tag{7}$$

where, $F(t)$, F^0, and $G(t,F(t))$ are defined as follows:

$$F(t) = \begin{Bmatrix} S(t) \\ C(t) \\ Q(t) \\ E(t) \\ P(t) \end{Bmatrix}, \; F^0 = \begin{Bmatrix} S^0 \\ C^0 \\ Q^0 \\ E^0 \\ P^0 \end{Bmatrix} \quad \text{and} \quad G(t,F(t)) = \begin{Bmatrix} \Phi_1(t,S,C,Q,E,P) \\ \Phi_2(t,S,C,Q,E,P) \\ \Phi_3(t,S,C,Q,E,P) \\ \Phi_4(t,S,C,Q,E,P) \\ \Phi_5(t,S,C,Q,E,P) \end{Bmatrix}.$$

In view of Lemma 1, the solution of system (6) can be rewritten as

$$F(t) = F^0 + \frac{1}{\Gamma(\theta)} \int_0^t (t-\kappa)^{\theta-1} G(\kappa, F(\kappa)) d\kappa.$$

The operator $\mathbb{T}$ is considered for further work:

$$\mathbb{T}F(t) = F^0 + \frac{1}{\Gamma(\theta)} \int_0^t (t-\kappa)^{\theta-1} G(\kappa, F(\kappa)) d\kappa. \tag{8}$$

The following assumptions are helpful in understanding theorems and rest of the paper:

(A_1) For $F_1, F_2 \in \mathbf{W}$, we have $a_G > 0$ such that:

$$\big\|G(F_1) - G(F_2)\big\| \leq a_G \|F_1 - F_2\|.$$

(A_2) For $F \in \mathbf{W}$, we have $b_G, c_G > 0$ such that:

$$\big\|G(F)\big\| \leq b_G \|F\| + c_G.$$

Theorem 2. *Suppose that the assumption* (A_1) *holds along with considering the inequality* $a_G \varpi^\theta < \Gamma(\theta+1)$. *Then, the problem* (6) *exhibits a unique solution.*

Proof. Consider $F_1, F_2 \in \mathbf{W}$, one can write

$$\begin{aligned}
\|\mathbb{T}F_1 - \mathbb{T}F_2\| &= \max_{t\in J}\Bigg\{ \frac{1}{\Gamma(\theta)} \Bigg\{ \int_0^t (t-\kappa)^{\theta-1} G(\kappa, F_1(\kappa)) d\kappa \\
&\quad - \int_0^t (t-\kappa)^{\theta-1} G(\kappa, F_2(\kappa)) d\kappa \Bigg\} \Bigg\} \\
&\leq \max_{t\in J}\Bigg\{ \frac{1}{\Gamma(\theta)} \Bigg\{ \int_0^t (t-\kappa)^{\theta-1} \left| G(\kappa, F_1(\kappa)) \right. \\
&\quad \left. - G(\kappa, F_2(\kappa)) \right| d\kappa \Bigg\} \Bigg\} \\
&\leq \max_{t\in J}\Bigg\{ \frac{a_G t^\theta}{\Gamma(\theta+1)} |F_1 - F_2| \Bigg\}
\end{aligned}$$

$$\leq \frac{a_G \varpi^\theta}{\Gamma(\theta+1)} \|F_1 - F_2\|.$$

Hence, $\mathbb{T}$ has a unique solution. ■

Theorem 3. *Let us consider that assumptions* (A_1, A_2) *are true, then there exists at least one solution of the system* (6).

Proof. To prove that $\mathbb{T} : \mathbf{W} \to \mathbf{W}$ satisfies the condition of Schaudar fixed point theorem, we suppose a closed convex subset $\mathbb{B} = \{F \in \mathbf{W} : \|F\| \leq r\}$. Moreover, the proof is divided in the following steps:
Step–1 (Continuity of the operator $\mathbb{T}$): Let us suppose a sequence F_n such that $F_n \to F$ and $t \in J$, we consider

$$\begin{aligned}
\|\mathbb{T}F_n - \mathbb{T}F\| &= \max_{t\in J}\left\{\frac{1}{\Gamma(\theta)}\left\{\int_0^t (t-\kappa)^{\theta-1} G(\kappa, F_n(\kappa))d\kappa\right.\right. \\
&- \left.\left.\int_0^t (t-\kappa)^{\theta-1} G(\kappa, F(\kappa))d\kappa\right\}\right\} \\
&\leq \max_{t\in J}\left\{\frac{1}{\Gamma(\theta)}\left\{\int_0^t (t-\kappa)^{\theta-1} |G(\kappa, F_n(\kappa))\right.\right. \\
&\left.\left. -G(\kappa, F(\kappa))| d\kappa\right\}\right\} \\
&\leq \max_{t\in J}\left\{\frac{a_G t^\theta}{\Gamma(\theta+1)}|F_n - F|\right\} \leq \frac{a_G \varpi^\theta}{\Gamma(\theta+1)}\|F_n - F\|.
\end{aligned}$$

Hence, $\|\mathbb{T}F_n - \mathbb{T}F\| \to 0$ as $n \to \infty$ proves that $\mathbb{T}$ is continuous.

Step–2 (Boundedness of the operator $\mathbb{T}$): The image of the bounded set under $\mathbb{T}$ is bounded in $\mathbf{W}$. Mathematically,

$$\begin{aligned}
\|\mathbb{T}F\| &= \max_{t\in J}\left|F^0 + \frac{1}{\Gamma(\theta)}\int_0^t (t-\kappa)^{\theta-1} G(\kappa, F(\kappa))d\kappa\right| \\
&\leq \max_{t\in J}\left\{|F^0| + \frac{1}{\Gamma(\theta)}\int_0^t (t-\kappa)^{\theta-1}|G(\kappa, F(\kappa))|d\kappa\right\}
\end{aligned}$$

$$\leq \quad F^0 + \frac{(b_G r + c_G)}{\Gamma(\theta+1)},$$

where $||F|| \leq r$, which shows that $\mathbb{T}$ is bounded.
Step–3 (Equi-continuity of the operator $\mathbb{T}$): Let $t_1, t_2 \in J$, such that $t_1 < t_2$. Then, the norm gives

$$\begin{aligned}
\|\mathbb{T}F(t_1) - \mathbb{T}F(t_2)\| &= \max_{t\in J}\Big|\frac{1}{\Gamma(\theta)}\int_0^{t_1}(t_1-\kappa)^{\theta-1}G(\kappa,F(\kappa))d\kappa \\
&- \frac{1}{\Gamma(\theta)}\int_0^{t_2}(t_2-\kappa)^{\theta-1}G(\kappa,F(\kappa))d\kappa\Big| \\
&= \max_{t\in J}\Big|\frac{1}{\Gamma(\theta)}\int_0^{t_1}(t_1-\kappa)^{\theta-1}G(\kappa,F(\kappa))d\kappa \\
&- \frac{1}{\Gamma(\theta)}\int_0^{t_1}(t_2-\kappa)^{\theta-1}G(\kappa,F(\kappa))d\kappa \\
&- \frac{1}{\Gamma(\theta)}\int_{t_1}^{t_1}(t_2-\kappa)^{\theta-1}G(\kappa,F(\kappa))d\kappa\Big| \\
&\leq \frac{b_G r + c_G}{\Gamma(\theta+1)}\left\{\left({t_1}^{\theta} - {t_2}^{\theta}\right) + (t_2-t_1)^{\theta} - (t_2-t_1)^{\theta}\right\}.
\end{aligned}$$

Applying limit $t_1 \to t_2$ to get $\|\mathbb{T}F(t_1) - \mathbb{T}F(t_2)\| \to 0$. Steps 1–3 are the desired results of the Schaudar fixed point theorem, $\mathbb{T}$ is equi-continuous, and consequently, problem (6) has at least one solution. ■

3 Results and discussion

In this part, we obtained the approximate solutions of the system (2) through Euler method and LADM. After finding the approximate solutions, we briefly discuss the behavior of their obtained solutions with the aid of two- and three-dimensional plots. A comparative study is also provided in the current section with the help of tables for various values of the fractional-order.

3.1 Solutions with Euler method

In this subsection, we get the solution of the concerned problem with the help of the Euler method. First, we obtain the numerical solutions, and then using MATLAB, the numerical simulations are obtained. The Euler scheme for system (2) is given as follows:

$$\begin{cases} S(t_{i+1}) = S(t_i) + \dfrac{h^\theta}{\Gamma(\theta+1)} \left\{ -\alpha S(t_i) E(t_i) + \beta C(t_i) - \omega S(t_i) C(t_i) + \eta Q(t_i) \right\}, \\ C(t_{i+1}) = C(t_i) + \dfrac{h^\theta}{\Gamma(\theta+1)} \left\{ \alpha S(t_i) E(t_i) - (\beta+\gamma) C(t_i) - \omega S(t_i) C(t_i) + (\eta+\sigma) Q(t_i) \right\}, \\ Q(t_{i+1}) = Q(t_i) + \dfrac{h^\theta}{\Gamma(\theta+1)} \left\{ \omega S(t_i) C(t_i) - (\eta+\sigma) Q(t_i) \right\}, \\ E(t_{i+1}) = E(t_i) + \dfrac{h^\theta}{\Gamma(\theta+1)} \left\{ -\alpha S(t_i) E(t_i) + (\beta+\gamma) C(t_i) \right\}, \\ P(t_{i+1}) = P(t_i) + \dfrac{h^\theta}{\Gamma(\theta+1)} \left\{ \gamma C(t_i) + \sigma Q(t_i) \right\}. \end{cases} \tag{9}$$

In Eq. (9), h is the step size defined as: $t_{i+1} = t_i + h$ for $i = 0, 1, 2, 3, \cdots, \lambda$. One can get the classical Euler scheme by putting $\theta = 1$ into system (9). We consider the initial values $S^0 = 0.6$, $E^0 = 0.4$ and $C^0 = Q^0 = P^0 = 0$ to obtain the approximate solution.

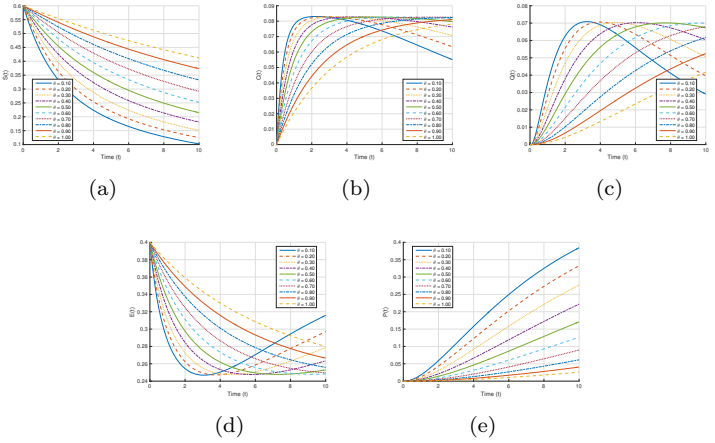

Figure 1. Investigating $S(t)$, $C(t)$, $Q(t)$, $E(t)$, $P(t)$ visually for various values of θ and parameter values $\alpha = 0.1$, $\beta = 0.05$, $\gamma = 0.03$, $\omega = 0.2$, $\eta = 0.01$, $\sigma = 0.05$, $h = 0.1$.

In Fig. 1, the solutions obtained through the Euler method are presented. It is observed in Figs. 1(a)–(c) that after decreasing the fractional

orders, the solutions tends to a stable direction, which confirms the importance of the fractional dynamics in enzymatic processes. In Fig.

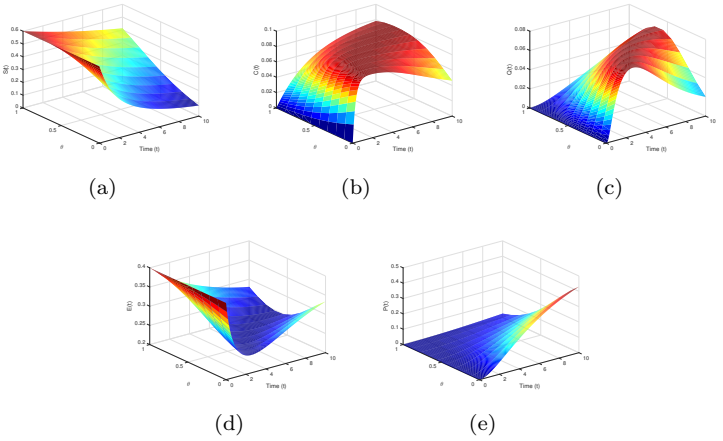

Figure 2. Concentration dynamics of all species $S(t)$, $C(t)$, $Q(t)$, $E(t)$, and $P(t)$ as functions of time t and fractional order θ, with fixed reaction parameters $\alpha = 0.1$, $\beta = 0.05$, $\gamma = 0.03$, $\omega = 0.2$, $\eta = 0.01$, $\sigma = 0.05$, and step size $h = 0.1$

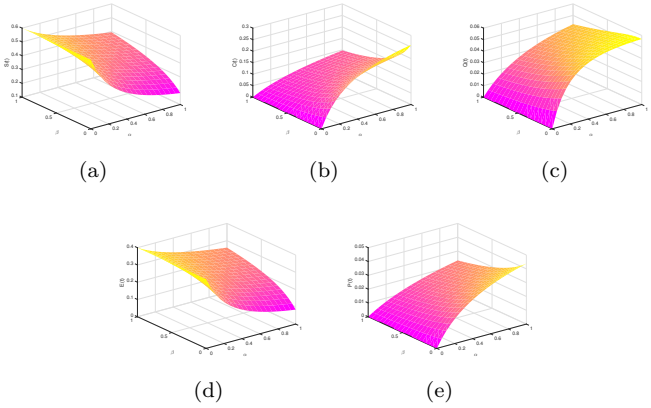

Figure 3. Concentration profiles of the fractional-order enzymatic reaction model against reaction parameters α and β, with fixed values $t = 5$, $\theta = 0.95$, $\gamma = 0.03$, $\omega = 0.2$, $\eta = 0.01$, $\sigma = 0.05$, and $h = 0.1$.

2, the variations in concentrations with respect to the fractional order θ are plotted. One can see the natural phenomena of the reaction with the advancement in time, the concentrations of $S(t)$ and $E(t)$ decrease while $P(t)$ and $Q(t)$ increase. The concentration of $C(t)$ shows a trend of increase before attaining steady state. The fractional order parameter introduces distinctive dynamics to the solutions and expands the range of possible behaviors beyond what is achievable with integer-order models. Moreover, in Figs. 3–5, we illustrated geometrical representations of the solutions, where the concentrations are plotted against randomly selected reaction parameters.

In Fig. 3, the concentrations against the reaction parameters α and β are provided. The cooperative nature of the reaction reveals that these parameters exert a significant impact during the early phase of the process. The parameter α specifies the initial binding affinity, while β regulates the turnover rate of the reaction. It is observed that significant changes-particularly in the concentrations of substrate and enzyme—occur with variations in α and β, affecting the stability of the enzymatic process.

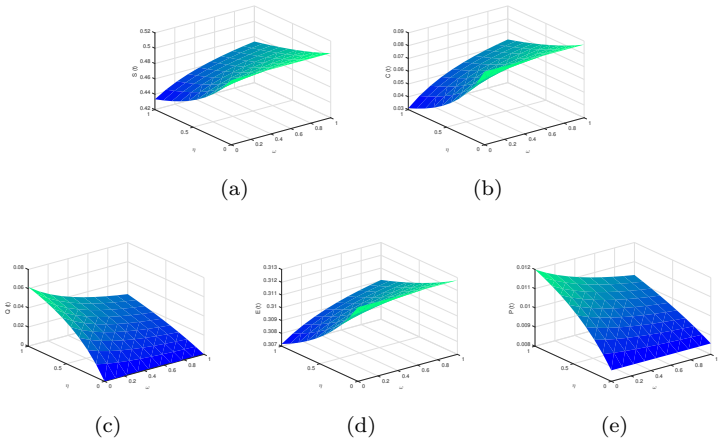

Figure 4. Response of substrate, enzyme, and product concentrations to variations in cooperative parameters ω and η, evaluated at $t = 5$ and $\theta = 0.95$, under fixed kinetic constants $\alpha = 0.1$, $\beta = 0.05$, $\gamma = 0.03$, $\sigma = 0.05$, and step size $h = 0.1$.

In a similar fashion, ω and η have the same impact on the enzyme kinetics as shown in Fig. 4. Similarly, the usage of cooperative phenomena on the parameters ω and η control in the third stage of the reaction and have a great impact on the concentrations of substrate and complex enzyme-substrate. As these mentioned parameters vary, the total activity of the solutions or concentrations changes. It is clear from the reaction that we

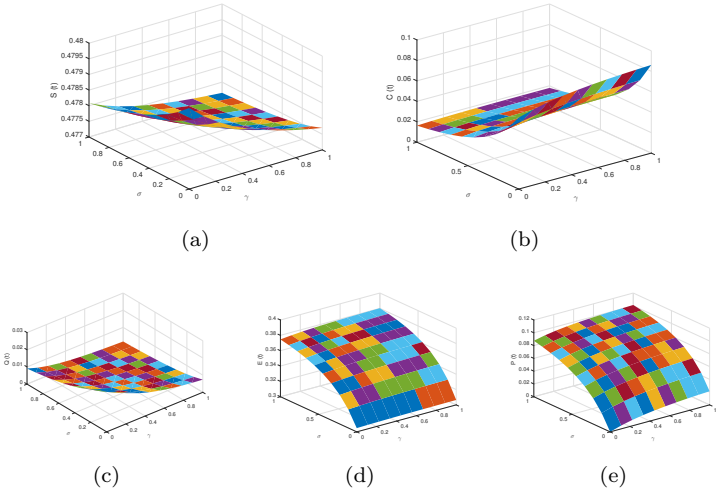

Figure 5. Response of $S(t)$, $C(t)$, $Q(t)$, $E(t)$, and $P(t)$ to variations in γ and σ, at $t = 5$ and $\theta = 0.95$, with $\alpha = 0.1$, $\beta = 0.05$, $\omega = 0.2$, $\eta = 0.01$, $h = 0.1$.

have taken these parameters randomly just for the readers to show visually the impact of these parameters on the concentrations in the reactions.

In this regard, the solutions of the system (2) are provided in Fig. 5. The parameter γ has an impact on the concentrations of complex enzyme-substrate, product, and enzyme. The parameter σ has a direct impact on the concentrations of dual bound substrate-enzyme, complex substrate-enzyme, and product. The impacts of these parameters on the dynamics of the reaction are clear from the aforementioned figure. Thus, from Figs. 1–5, it is obvious that these reaction parameters (α, β, γ, σ, ω, η) have a versatile nature of the solutions on the enzymatic reaction dynamics in the presence of fractional order.

3.2 LADM solutions

This subsection presents the solution of system (2) obtained through the Laplace–Adomian decomposition method (LADM). Moreover, we have provided the approximate solutions along with complete geometrical interpretation for better analysis.

We begin by applying the Laplace transform (5) to the first equation of system (2) to obtain:

$$\mathbb{L}\{S(t)\} = \frac{S(0)}{s} + \frac{1}{s^{\theta}}\mathbb{L}\left\{-\alpha S(t)E(t) + \beta C(t) - \omega S(t)C(t) + \eta Q(t)\right\}. \tag{10}$$

Using the initial condition, Eq. (10) becomes

$$\mathbb{L}\{S(t)\} = \frac{S^0}{s} + \frac{1}{s^{\theta}}\mathbb{L}\left\{-\alpha S(t)E(t) + \beta C(t) - \omega S(t)C(t) + \eta Q(t)\right\}. \tag{11}$$

Applying inverse transformation on the Eq. (11) to achieve

$$S(t) = S^0 + \mathbb{L}^{-1}\left\{\frac{1}{s^{\theta}}\mathbb{L}\left\{-\alpha S(t)E(t) + \beta C(t) - \omega S(t)C(t) + \eta Q(t)\right\}\right\}. \tag{12}$$

For further calculations, we consider

$$S = \sum_{n=0}^{\infty} S_n, C = \sum_{n=0}^{\infty} C_n, SE = \sum_{n=0}^{\infty} \mathbb{A}_n, SC = \sum_{n=0}^{\infty} \mathbb{B}_n.$$

The equations $\mathbb{A}_n$ and $\mathbb{B}_n$ are given as follows:

$$\mathbb{A}_n = \frac{1}{\Gamma(n+1)}\frac{d^n}{d\mu^n}\left[\left(\left(\sum_{j=0}^{n}\mu^j S_j\right)\left(\sum_{j=0}^{n}\mu^j E_j\right)\right)\right]_{\mu=0},$$

$$\mathbb{B}_n = \frac{1}{\Gamma(n+1)}\frac{d^n}{d\mu^n}\left[\left(\left(\sum_{j=0}^{n}\mu^j S_j\right)\left(\sum_{j=0}^{n}\mu^j C_j\right)\right)\right]_{\mu=0}.$$

Substituting these values into Eq. (12) yields:

$$\sum_{n=0}^{\infty} S_n(t) = S^0 + \mathbb{L}^{-1}\left\{\frac{1}{s^\theta}\mathbb{L}\left\{-\alpha\mathbb{A}_n + \beta\sum_{n=0}^{\infty} C_n - \omega\mathbb{B}_n + \eta\sum_{n=0}^{\infty} Q_n\right\}\right\}.$$

From the preceding equation, we get

$$S_0 = S^0, \quad S_1 = \mathbb{L}^{-1}\left\{\frac{1}{s^\theta}\mathbb{L}\left\{-\alpha\mathbb{A}_0 + \beta C_0 - \omega\mathbb{B}_0 + \eta Q_0\right\}\right\},$$

and so forth. The generic form can be written as:

$$S_{n+1} = \mathbb{L}^{-1}\left\{\frac{1}{s^\theta}\mathbb{L}\left\{-\alpha\mathbb{A}_n + \beta C_n - \omega\mathbb{B}_n + \eta Q_n\right\}\right\}, \ n \geq 0.$$

The solution is computed iteratively: starting with S_0, we obtain S_1, S_2, and so on, leading to the series solution $S = S_0 + S_1 + S_2 + \cdots$. Applying the same approach to the remaining equations, we find:

$$\begin{cases}
C_0 = C^0, \quad C_1 = \mathbb{L}^{-1}\left\{\frac{1}{s^\theta}\mathbb{L}\left\{\alpha\mathbb{A}_0 - (\beta+\gamma)C_0 - \omega\mathbb{B}_0 + (\eta+\sigma)Q_0\right\}\right\}, \\
C_{n+1} = \mathbb{L}^{-1}\left\{\frac{1}{s^\theta}\mathbb{L}\left\{\alpha\mathbb{A}_n - (\beta+\gamma)C_n - \omega\mathbb{B}_n + (\eta+\sigma)Q_n\right\}\right\}, \ n \geq 0, \\
Q_0 = Q^0, \quad Q_1 = \mathbb{L}^{-1}\left\{\frac{1}{s^\theta}\mathbb{L}\left\{\omega\mathbb{B}_0 - (\eta+\sigma)Q_0\right\}\right\}, \\
Q_{n+1} = \mathbb{L}^{-1}\left\{\frac{1}{s^\theta}\mathbb{L}\left\{\omega\mathbb{B}_n - (\eta+\sigma)Q_n\right\}\right\}, \ n \geq 0, \\
E_0 = E^0, \quad E_1 = \mathbb{L}^{-1}\left\{\frac{1}{s^\theta}\mathbb{L}\left\{-\alpha\mathbb{A}_0 + (\beta+\gamma)C_0\right\}\right\}, \\
E_{n+1} = \mathbb{L}^{-1}\left\{\frac{1}{s^\theta}\mathbb{L}\left\{-\alpha\mathbb{A}_n + (\beta+\gamma)C_n\right\}\right\}, \ n \geq 0, \\
P_0 = P^0, \quad P_1 = \mathbb{L}^{-1}\left\{\frac{1}{s^\theta}\mathbb{L}\left\{\gamma C_0 + \sigma Q_0\right\}\right\}, \\
P_{n+1} = \mathbb{L}^{-1}\left\{\frac{1}{s^\theta}\mathbb{L}\left\{\gamma C_n + \sigma Q_n\right\}\right\}, \ n \geq 0.
\end{cases}$$

To get more specific and approximate solution from the above general solution. Consider the same initial values ($S^0 = 0.6$, $E^0 = 0.4$, $C^0 = Q^0 =$

$P^0 = 0$) of Euler method, and applying the above procedure, one may get the following approximate solution of the specified model (2):

$$\begin{cases} S(t) = 0.6 - \dfrac{0.24\alpha t^{\theta}}{\Gamma(\theta+1)} + (0.24\alpha + 0.24\alpha\beta - 0.144\omega)\dfrac{t^{2\theta}}{\Gamma(2\theta+1)}, \\ C(t) = \dfrac{0.24\alpha t^{\theta}}{\Gamma(\theta+1)} - 0.24\alpha - 0.24\alpha(\beta+\gamma) - 0.144\alpha\omega\dfrac{t^{2\theta}}{\Gamma(2\theta+1)}, \\ Q(t) = \dfrac{0.144\alpha\omega t^{2\theta}}{\Gamma(2\theta+1)}, \\ E(t) = 0.4 - \dfrac{0.24\alpha t^{\theta}}{\Gamma(\theta+1)} + (0.24\alpha + 0.24\alpha(\beta+\gamma)\dfrac{t^{2\theta}}{\Gamma(2\theta+1)}, \\ P(t) = \dfrac{0.24\alpha\gamma t^{2\theta}}{\Gamma(2\theta+1)}. \end{cases} \tag{13}$$

In solution (13), we present the first three terms for each component of the transformed model. A more precise approximation of the dynamics of the considered model can be achieved by including additional terms using the procedure described above. To properly understand the physical and geometrical interpretation of the cooperative enzymatic reaction described by system (2), we present the following visualizations along with complete descriptions.

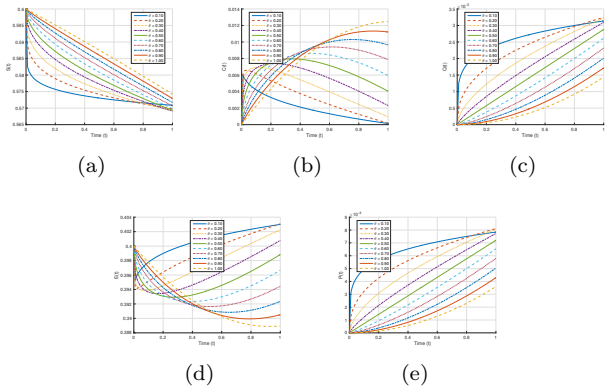

Figure 6. Effect of fractional order θ on $S(t)$, $C(t)$, $Q(t)$, $E(t)$, and $P(t)$, with fixed kinetic constants $\alpha = 0.1$, $\beta = 0.05$, $\gamma = 0.03$, $\omega = 0.2$.

Two-dimensional plots of the concentrations for the model under consideration are presented in Fig. 6. These solutions are calculated through LADM for a few terms, and the accuracy of these solutions can be increased. This is the reason that the solution attained through Euler method are better in comparison. Additionally, it can be seen that at lower fractional-orders, the curves show more stable trends, reflecting the memory effect in fractional-order models. The graphical analysis presents generalized framework for modeling biochemical processes in reality, pointing out the significance of FC in chemical reaction modeling.

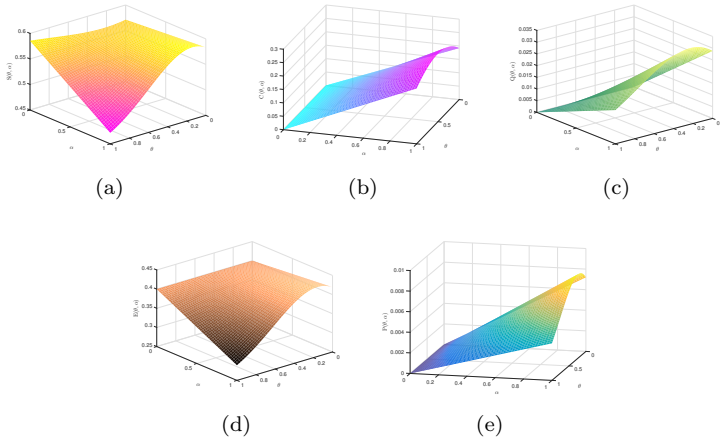

Figure 7. Three-dimensional visualization of S, C, Q, E, and P against fractional order θ and binding rate α, for $\beta = 0.05$, $t = 1$, $\gamma = 0.03$, $\omega = 0.2$.

Figure 7 shows the three-dimensional representation of the solutions calculated through LADM against the fractional order θ and reaction parameter α. These plots give further information about how these two parameters can affect the dynamics of the biochemical system. The surface plots demonstrate that the substrate and enzyme concentrations typically diminish with growing θ and α, while the product and complex concentrations grow, which serves to reflect the enzyme kinetics.

3.3 Neural network approximation

To assess the accuracy of the suggested approach utilizing a Levenberg-Marquardt neural network environment backed by regression analysis and error distribution statistics, data is segregated into training (70%), validation (15%), and testing (15%) sets. In this section, we consider data similar to that in Fig. 1 to perform simulations.

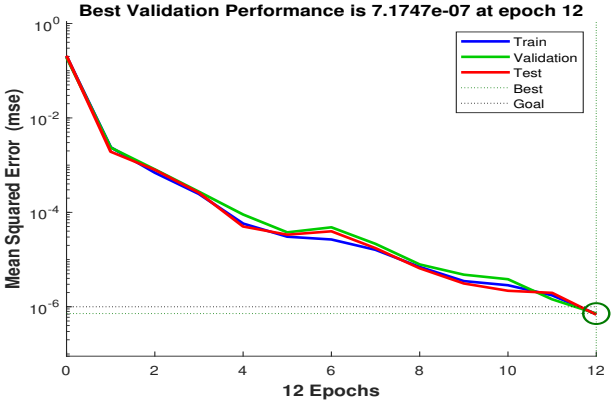

Figure 8. Mean squared error (MSE) training performance across 12 epochs for the neural network approximation of the fractional-order enzymatic model.

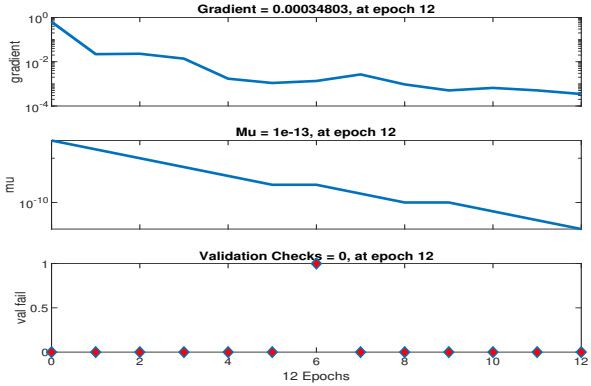

Figure 9. Training state metrics (gradient, validation checks, and mu parameter) during the 12-epoch training process.

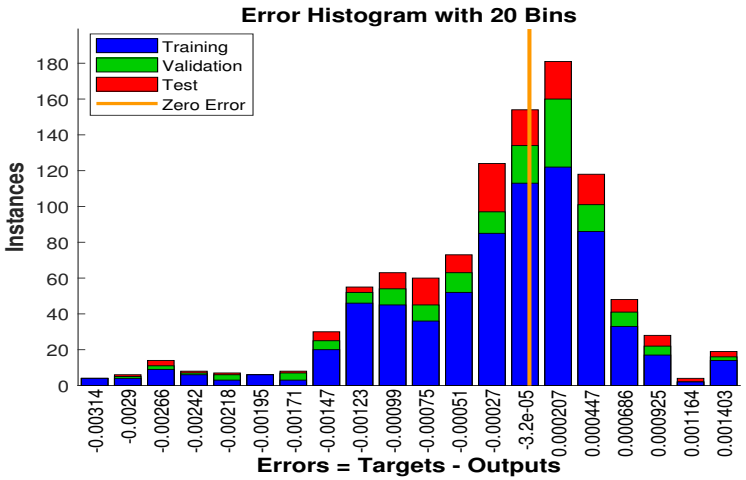

Figure 10. Error histogram showing the distribution of prediction errors across training, validation, and test datasets after 12 epochs.

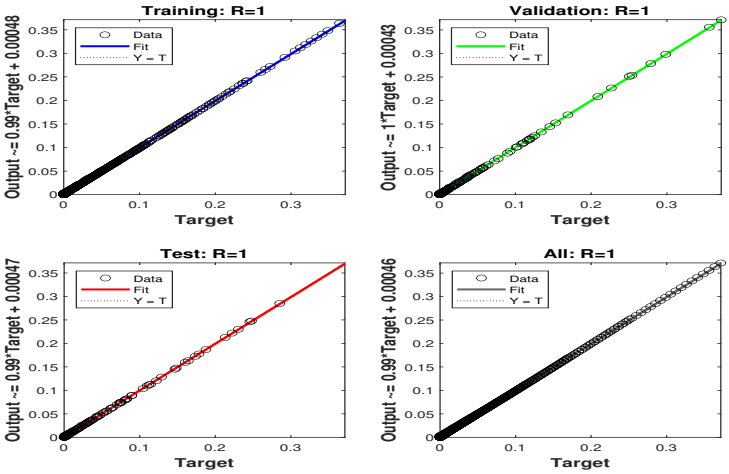

Figure 11. Regression plots comparing neural network predictions against target values for training, validation, test, and overall datasets.

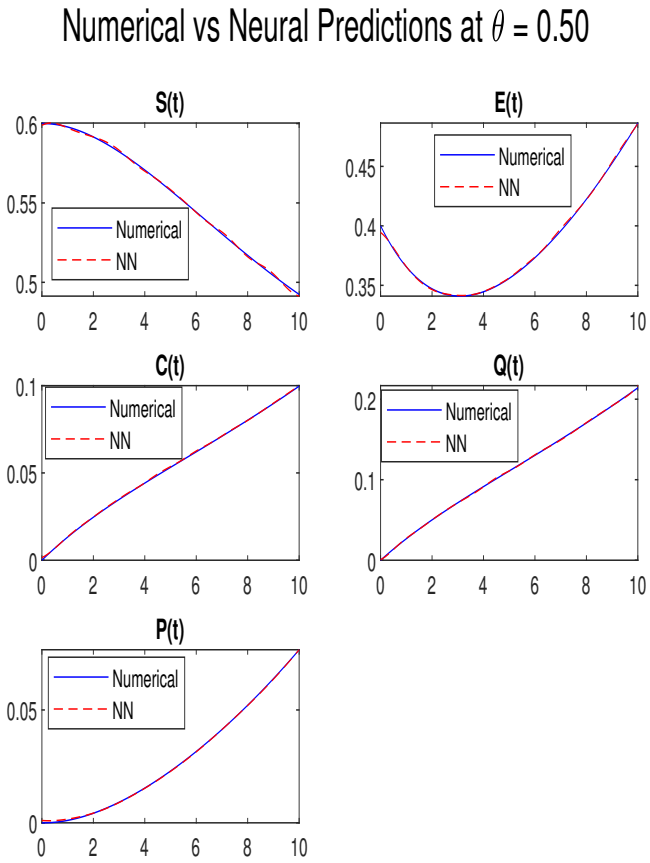

Figure 12. Comparison of numerical solutions and neural network predictions for $S(t)$, $C(t)$, $Q(t)$, $E(t)$, and $P(t)$ at $\theta = 0.50$ after 12 training epochs.

Figures 8–12 provide illustrations of the MSE performance and training tests of the model (2) for $\theta = 0.5$.

3.4 Comparison of LADM and Euler method solutions

The following tables present a comparative analysis of the solutions for the variables $S(t)$, $E(t)$, $C(t)$, $Q(t)$, and $P(t)$ obtained using both the

Euler and LADM methods. In order to demonstrate the effect of varying fractional-orders, three separate tables for three different fractional-orders are provided. The results in these tables signify how the result changes with the change in fractional-order.

Time	S_LADM	S_Euler	E_LADM	E_Euler	C_LADM	C_Euler	Q_LADM	Q_Euler	P_LADM	P_Euler
0.0	0.6000	0.6000	0.4000	0.4000	0.0000000	0.0000000	0.0000000	0.0000000	0.0000000	0.0000000
0.1	0.5976	0.59758	0.3976	0.39773	0.0024000	0.0022848	0.0000000	0.0000144	0.0000000	0.0000036
0.2	0.59521	0.59513	0.39524	0.39572	0.0047282	0.0043392	0.0000287	0.0000576	0.0000072	0.0000144
0.3	0.59282	0.59264	0.39293	0.39397	0.0069868	0.0061632	0.0000848	0.0001296	0.0000215	0.0000324
0.4	0.59044	0.59011	0.39065	0.39247	0.0091779	0.0077568	0.0001671	0.0002304	0.0000429	0.0000576
0.5	0.58808	0.58755	0.38842	0.39124	0.0113040	0.0091200	0.0002745	0.0003600	0.0000713	0.0000900
0.6	0.58572	0.58495	0.38623	0.39027	0.0133660	0.0102530	0.0004058	0.0005184	0.0001066	0.0001296
0.7	0.58336	0.58232	0.38407	0.38955	0.0153670	0.0111550	0.0005600	0.0007056	0.0001487	0.0001764
0.8	0.58102	0.57965	0.38196	0.38909	0.0173090	0.0118270	0.0007359	0.0009216	0.0001976	0.0002304
0.9	0.57869	0.57694	0.37987	0.38890	0.0191930	0.0122690	0.0009326	0.0011664	0.0002532	0.0002916
1.0	0.57637	0.57420	0.37783	0.38896	0.0210210	0.0124800	0.0011491	0.0014400	0.0003154	0.0003600
1.1	0.57405	0.57142	0.37582	0.38928	0.0227950	0.0124610	0.0013846	0.0017424	0.0003842	0.0004356
1.2	0.57175	0.56861	0.37385	0.38986	0.0245170	0.0122110	0.0016380	0.0020736	0.0004596	0.0005184
1.3	0.56945	0.56576	0.37190	0.39070	0.0261880	0.0117310	0.0019085	0.0024336	0.0005413	0.0006084
1.4	0.56717	0.56287	0.37000	0.39180	0.0278090	0.0110210	0.0021953	0.0028224	0.0006294	0.0007056
1.5	0.56490	0.55995	0.36812	0.39316	0.0293830	0.0100800	0.0024976	0.0032400	0.0007238	0.0008100
1.6	0.56264	0.55699	0.36627	0.39478	0.0309100	0.0089088	0.0028146	0.0036864	0.0008244	0.0009216
1.7	0.56038	0.55400	0.36446	0.39665	0.0323930	0.0075072	0.0031455	0.0041616	0.0009313	0.0010404
1.8	0.55814	0.55097	0.36268	0.39879	0.0338320	0.0058752	0.0034897	0.0046656	0.0010442	0.0011664
1.9	0.55592	0.54790	0.36092	0.40119	0.0352290	0.0040128	0.0038464	0.0051984	0.0011631	0.0012996
2.0	0.55370	0.54480	0.35920	0.40384	0.0365850	0.0019200	0.0042150	0.0057600	0.0012880	0.0014400

Table 1. Comparison of both methods at $\theta = 1.0$, $\alpha = 0.1$, $\beta = 0.05$, $\gamma = 0.03$, $\omega = 0.2$, $\eta = 0.01$, and $\sigma = 0.05$.

Time	S_LADM	S_Euler	E_LADM	E_Euler	C_LADM	C_Euler	Q_LADM	Q_Euler	P_LADM	P_Euler
0.0	0.60000	0.60000	0.40000	0.40000	0.00000	0.00000	0.00000	0.00000	0.00000	0.00000
0.1	0.59725	0.59723	0.39725	0.39743	0.0027481	0.0025894	0.00000	0.000019841	0.00000	0.0000049603
0.2	0.59451	0.5946	0.39456	0.39536	0.0054021	0.0047166	0.000037588	0.00007405	0.0000094403	0.000018513
0.3	0.59178	0.592	0.39192	0.39364	0.0079653	0.0065238	0.00011088	0.00015999	0.000028213	0.000039998
0.4	0.58907	0.5894	0.38934	0.39223	0.010441	0.0080455	0.00021807	0.00027637	0.00005621	0.000069091
0.5	0.58636	0.58679	0.38681	0.39112	0.012832	0.0092999	0.00035742	0.00042229	0.000093325	0.00010557
0.6	0.58366	0.58418	0.38433	0.3903	0.015142	0.010299	0.00052728	0.00059711	0.00013945	0.00014928
0.7	0.58098	0.58155	0.3819	0.38975	0.017373	0.011051	0.00072605	0.00080031	0.00019449	0.00020008
0.8	0.57831	0.5789	0.37952	0.38947	0.019528	0.011563	0.00095221	0.0010314	0.00025832	0.00025786
0.9	0.57565	0.57623	0.37719	0.38945	0.02161	0.011839	0.0012043	0.0012901	0.00033086	0.00032253
1.0	0.573	0.57354	0.3749	0.38969	0.023622	0.011884	0.0014809	0.001576	0.00041199	0.00039401
1.1	0.57037	0.57082	0.37265	0.39019	0.025566	0.011703	0.0017807	0.0018889	0.00050161	0.00047223
1.2	0.56775	0.56809	0.37045	0.39093	0.027444	0.011297	0.0021024	0.0022285	0.00059963	0.00055713
1.3	0.56515	0.56533	0.3683	0.39193	0.029258	0.010669	0.0024448	0.0025945	0.00070594	0.00064864
1.4	0.56255	0.56255	0.36618	0.39316	0.031012	0.0098231	0.0028067	0.0029868	0.00082044	0.00074671
1.5	0.55998	0.55974	0.36411	0.39464	0.032706	0.0087602	0.0031869	0.0034052	0.00094304	0.0008513
1.6	0.55741	0.55691	0.36207	0.39637	0.034344	0.0074827	0.0035845	0.0038494	0.0010736	0.00096236
1.7	0.55487	0.55405	0.36008	0.39833	0.035926	0.0059924	0.0039982	0.0043194	0.0012121	0.0010798
1.8	0.55233	0.55117	0.35812	0.40052	0.037456	0.004291	0.0044273	0.0048149	0.0013584	0.0012037
1.9	0.54981	0.54826	0.3562	0.40296	0.038934	0.0023799	0.0048707	0.0053358	0.0015125	0.001334
2.0	0.54731	0.54533	0.35431	0.40562	0.040363	0.00026077	0.0053274	0.005882	0.0016741	0.0014705

Table 2. Comparison of both methods at $\theta = 0.95$, $\alpha = 0.1$, $\beta = 0.05$, $\gamma = 0.03$, $\omega = 0.2$, $\eta = 0.01$, and $\sigma = 0.05$.

Time	S_LADM	S_Euler	E_LADM	E_Euler	C_LADM	C_Euler	Q_LADM	Q_Euler	P_LADM	P_Euler
0.0	0.60000	0.60000	0.40000	0.40000	0.00000	0.00000	0.00000	0.00000	0.00000	0.00000
0.1	0.59686	0.59682	0.39686	0.3971	0.0031415	0.0029237	0.00000	0.000027226	0.00000	0.0000068066
0.2	0.59373	0.59402	0.39379	0.39499	0.0061601	0.0051038	0.000049088	0.000094808	0.000012337	0.000023702
0.3	0.59061	0.59131	0.39079	0.39333	0.0090607	0.0068704	0.00014445	0.0001967	0.000036848	0.000049176
0.4	0.58751	0.58865	0.38787	0.39203	0.011848	0.0082983	0.00028341	0.00033014	0.000073374	0.000082535
0.5	0.58442	0.58601	0.38501	0.39107	0.014527	0.0094259	0.00046342	0.00049333	0.00012176	0.00012333
0.6	0.58135	0.58339	0.38222	0.39041	0.017101	0.010278	0.00068204	0.00068496	0.00018183	0.00017124
0.7	0.5783	0.58077	0.37949	0.39003	0.019576	0.01087	0.00093696	0.000904	0.00025345	0.000226
0.8	0.57526	0.57815	0.37682	0.38993	0.021955	0.011217	0.001226	0.0011496	0.00033646	0.0002874
0.9	0.57223	0.57553	0.37421	0.39009	0.024241	0.011328	0.001547	0.0014211	0.0004307	0.00035528
1.0	0.56923	0.5729	0.37166	0.39051	0.026439	0.011211	0.001898	0.0017179	0.00053601	0.00042947
1.1	0.56624	0.57026	0.36917	0.39117	0.028553	0.010874	0.0022771	0.0020394	0.00065226	0.00050984
1.2	0.56327	0.56761	0.36673	0.39206	0.030584	0.010323	0.0026824	0.0023852	0.00077929	0.00059629
1.3	0.56032	0.56496	0.36435	0.39319	0.032538	0.0095619	0.0031124	0.0027548	0.00091695	0.0006887
1.4	0.55739	0.56229	0.36202	0.39455	0.034417	0.0085966	0.0035652	0.0031479	0.0010651	0.00078698
1.5	0.55447	0.5596	0.35974	0.39613	0.036224	0.0074306	0.0040394	0.0035641	0.0012236	0.00089104
1.6	0.55158	0.5569	0.35751	0.39794	0.037961	0.0060678	0.0045335	0.0040032	0.0013923	0.0010008
1.7	0.5487	0.55419	0.35532	0.39995	0.039632	0.0045114	0.0050461	0.0044648	0.001571	0.0011162
1.8	0.54585	0.55146	0.35318	0.40218	0.04124	0.0027645	0.0055758	0.0049486	0.0017597	0.0012371
1.9	0.54301	0.54872	0.35109	0.40462	0.042786	0.00082991	0.0061213	0.0054544	0.0019581	0.0013636
2.0	0.5402	0.54596	0.34905	0.40727	0.044273	0.00082990	0.0066815	0.005982	0.0021662	0.0014955

Table 3. Comparison of both methods at $\theta = 0.90$, $\alpha = 0.1$, $\beta = 0.05$, $\gamma = 0.03$, $\omega = 0.2$, $\eta = 0.01$, and $\sigma = 0.05$.

Tables 1, 2, and 3 present a comparative analysis of the LADM and Euler solutions for different fractional orders θ. In Table 1, where $\theta = 1$, both methods yield nearly identical results, demonstrating that LADM and the Euler scheme perform well in the classical integer-order case. However, one can see in Table 2 and Table 3 that for $\theta = 0.90$ and $\theta = 0.95$, a great variation occurs.

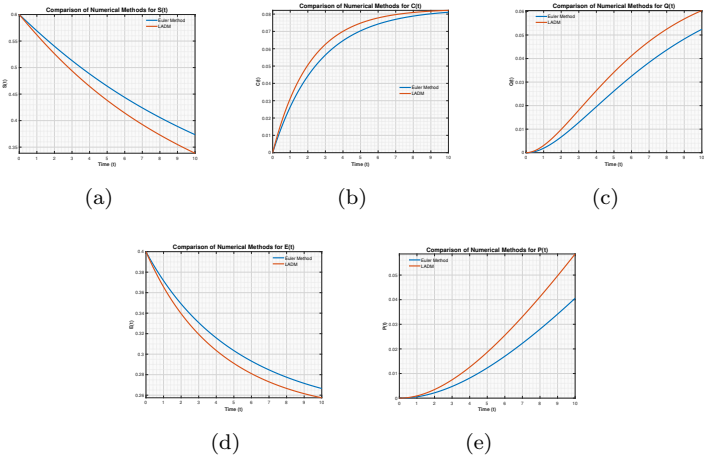

Figure 13. Investigating $S(t)$, $C(t)$, $Q(t)$, $E(t)$, $P(t)$ visually for fixed value of $\theta = 0.9$ and parameter values $\alpha = 0.1$, $\beta = 0.05$, $\gamma = 0.03$, $\omega = 0.2$, $\eta = 0.01$, $\sigma = 0.05$, $h = 0.1$.

Figure 13 presents a comparison between the solutions to system (2) obtained through the Euler scheme and LADM.
The LADM presents the approximate solutions which is valuable for initial validation and short-time insight. For detailed long time dynamical simulations, the Euler scheme is used as primary tool in our analysis. The Euler scheme is better suited for this analysis because of its straightforward implementation and efficiency of computation, as it avoids the complexity involved in obtaining high-order Adomian polynomials as required in LADM. The main point in our analysis at this time is the impact of fractional order on the solutions and how this will be beneficial for future work. This shows that fractional-order dynamics are more effective, making it more reliable for enzymatic reaction models.

4 Conclusion

We have developed a fractional-order cooperative enzymatic reaction model using the Liouville–Caputo derivative to extend classical enzymatic kinetics. We have investigated the existence and uniqueness of solutions through the theory of non-linear functional analysis. Numerical solutions of the proposed model have been obtained using the Euler method and the LADM. The accuracy of the proposed approach has been evaluated using a Levenberg-Marquardt neural network platform, supplemented with regression analysis and error distribution statistics. The data are split into training (70%), validation (15%), and testing (15%) sets. The approximate solutions have been analyzed graphically in detail using $2D$ and $3D$ plots under different fractional orders and reaction parameters. Moreover, a tabular presentation of a comparative analysis of numerical solutions for both integer and fractional orders has been provided, focusing on the influence of fractional differentiation over reaction kinetics. This creates an entirely new perspective on chemical reaction modeling where fractional derivatives are introduced to understand the dynamics of a reaction better. The results have deeper insight into enzyme kinetics, which can be further developed for pharmaceutical research, metabolic engineering, and optimization of biochemical processes. This study would therefore further

emphasis the precise optimization of reaction dynamics in biochemistry by FC. This would create a framework for future investigations into enzyme-substrate interaction, catalysis, and other complex biochemical networks, eventually advancing it in biomedical sciences and industrial applications.

***Acknowledgment*:** The authors extend their appreciation to the Deanship of Research and Graduate Studies at King Khalid University for funding this work through Large Group Project under grant number RGP 2/156/46.

References

[1] H. Alrabaiah, I. Ahmad, R. Amin, K. Shah, A numerical method for fractional variable order pantograph differential equations based on Haar wavelet, *Eng. Comput.* **38** (2022) 2655–2668.

[2] I. Ahmad, T. Abdeljawad, I. Mahariq, K. Shah, N. Mlaiki, G.U. Rahman, Iterative analysis of non-linear Swift–Hohenberg equations under non-singular fractional order derivative, *Results Phys.* **23** (2021) #104080.

[3] I. Ahmad, Z. Ali, B. Khan, K. Shah, T. Abdeljawad, Exploring the dynamics of Gumboro-Salmonella co-infection with fractal fractional analysis, *Alexandria Eng. J.* **117** (2025) 472–489.

[4] I. Ahmad, N. Ahmad, K. Shah, T. Abdeljawad, Some appropriate results for the existence theory and numerical solutions of fractals–fractional order malaria disease mathematical model, *Res. Control Optim.* **14** (2024) #100386.

[5] Ö.F. Akmecse, A novel random number generator and its application in sound encryption based on a fractional-order chaotic system, *J. Circ. Syst. Comput.* **32** (2023) #2350127.

[6] A. I. Amen, Integrability analysis of the smallest 3D biochemical reaction model, *MATCH Commun. Math. Comput. Chem.* **90** (2023) 333–356.

[7] T. Azizi, Application of the fractional calculus in pharmacokinetic compartmental modeling, *Commun. Biomath. Sci.* **5** (2022) 63–77.

[8] H. Bilal, R. A. Shah, H. Ahmad, A. Jan, T. Radwan, An intelligent framework for modeling nonlinear irreversible biochemical reactions using artificial neural networks, *Sci. Rep.* **15** (2025) #28458.

[9] M. Caputo, Linear models of dissipation whose Q is almost frequency independent–II, *Geophys. J. Int.* **13** (1967) 529–539.

[10] H. B. Chethan, N. Bin Turki, D. G. Prakasha, High performance computational approach to study model describing reversible two-step enzymatic reaction with time fractional derivative, *Sci. Rep.* **14** (2024) #21114.

[11] J. Chen, W. Sun, S. Zheng, Encrypting images using multiple fractional-order drive–response systems with practical finite-time synchronization, *Math. Comput. Simul.* **240** (2025) 423–437.

[12] R. E. Edwards, *Functional Analysis: Theory and Applications*, Courier Corporation, 2012.

[13] P. A. Frey, A. D. Hegeman, *Enzymatic Reaction Mechanisms*, Oxford Univ. Press, Oxford, 2007.

[14] B. Gao, A. Shukur, M. Marwan, N. Wang, On the complex dynamics of simple integer to fractional-order sine chaotic oscillators, *Fractals* (2025) #2550115.

[15] M.I. Gomoyunov, On viscosity solutions of path-dependent Hamilton–Jacobi–Bellman–Isaacs equations for fractional-order systems, *J. Diff. Eq.* **399** (2024) 335–362.

[16] X. Gao, Y. Jin, M. Marwan, F. Li, Y. Wei, Impact of Hopf and Bautin bifurcations on an auto catalytic chemical reaction system, *MATCH Commun. Math. Comput. Chem.* **94** (2025) 863–889.

[17] R. Golnik, P. F. Stadler, T. Gatter, Atom transition networks and isotope labeling patterns in large chemical reaction networks, *MATCH Commun. Math. Comput. Chem.* **95** (2026) 347–404.

[18] N. M. Goodey, S .J. Benkovic, Allosteric regulation and catalysis emerge via a common route, *Nat. Chem. Biol.* **4** (2008) 474–482.

[19] M. Izadi, H. Ahmad, H. M. Srivastava, Numerical computations of time-dependent auto-catalytic glycolysis chemical reaction-diffusion system, *MATCH Commun. Math. Comput. Chem.* **93** (2025) 69–97.

[20] A. Jan, R. A. Shah, H. Bilal, B. Almohsen, R. Jan, B. K. Sharma, Dynamics and stability analysis of enzymatic cooperative chemical reactions in biological systems with time-delayed effects, *Partial Differ. Equ. Appl. Math.* **11** (2024) #100850.

[21] A. Jan, R. A. Shah, H. Ahmad, H. Bilal, B. Almohsen, Dynamic behavior of enzyme kinetics cooperative chemical reactions, *AIP Adv.* **14** (2024) 0351391–03513912.

[22] M. Khan, Z. Ahmad, F. Ali, N. Khan, I. Khan, K. S. Nisar, Dynamics of two-step reversible enzymatic reaction under fractional derivative with Mittag-Leffler kernel, *PLoS One* **18** (2023) #e0277806.

[23] A. A. Kilbas, *Theory and Applications of Fractional Differential Equations*, Elsevier, Amsterdam, 2006.

[24] J. N. Kreikemeyer, K. Burrage, A. M. Uhrmacher, Discovering biochemical reaction models by evolving libraries, in: R. Gori, P. Milazzo, M. Tribastone (Eds.), *International Conference on Computational Methods in Systems Biology*, Springer, 2024, pp. 117–136.

[25] K. Kothari, Kajal, U. V. Mehta, R. Prasad, Fractional-order system modeling and its applications, *J. Eng. Sci. Technol. Rev.* **12** (2019) 1–10.

[26] J. Liu, R. Li, D. Huang, Stability, bifurcation and characteristics of chaos in a new commensurate and incommensurate fractional-order ecological system, *Math. Comput. Simul.* **236** (2025) 248–269.

[27] N. M. Mathavavisakan, K. Indhira, A mathematical approach to Ullmann reaction: ANFIS computing of a chemical retrial queue model under hybrid vacation, *MATCH Commun. Math. Comput. Chem.* **93** (2025) 99–128.

[28] A. E. Matouk, Applications of the generalized gamma function to a fractional-order biological system, *Heliyon* **9** (2023) #e18645.

[29] M. Marwan, G. Ali, F. Li, S. A. O. Abdallah, T. Saidani, Semi-analytical analysis of a fractional-order pandemic dynamical model using non-local operator, *Fractals* **33** (2025) #2550048.

[30] M. Marwan, A. Xiong, M. Han, R. Khan, Chaotic behavior of Lorenz-based chemical system under the influence of fractals, *MATCH Commun. Math. Comput. Chem.* **91** (2024) 307–336.

[31] J. C. Muriel, N. Cowie, S. T. Parkins, M. Mansouvar, T. Groves, L. K. NielsenShu, Visualization of high-dimensional biological pathways, *Bioinformatics* **40** (2024) #btae140.

[32] J. D. Murray, *Mathematical Biology: I. An Introduction*, Springer, New York, 2007.

[33] A. J. M. Ribeiro, I. G. Riziotis, J. D. Tyzack, N. Borkakoti, J. M. Thornton, EzMechanism: an automated tool to propose catalytic mechanisms of enzyme reactions, *Nat. Methods* **20** (2023) 1516–1522.

[34] K. Shah, I. Ahmad, Shafiullah, A. Mukheimer, T. Abdeljawad, M. B. Jeelani, On the existence and numerical simulation of Cholera epidemic model, *Open Phys.* **22** (2024) #20230165.

[35] K. Shah, T. Abdeljawad, On complex fractal-fractional order mathematical modeling of CO_2 emanations from energy sector, *Phys. Scr.* **99** (2023) #015226.

[36] K. Shah, T. Abdeljawad, A. Ali, Mathematical analysis of the Cauchy type dynamical system under piecewise equations with Caputo fractional derivative, *Chaos Solitons Fractals* **161** (2022) #112356.

[37] F. J. Sorcia-Vázquez, J. Y. Rumbo-Morales, J. A. Brizuela-Mendoza, G. Ortiz-Torres, E. Sarmiento-Bustos, A. F. Pérez-Vidal, E. M. Rentería-Vargas, M. De-la-Torre, R. Osorio-Sánchez, Experimental validation of fractional PID controllers applied to a two-tank system, *Mathematics* **11** (2023) #2651.

[38] J. Duan, X. Cheng, T. Deng, Topological isomers of DNA dodecahedral links, *MATCH Commun. Math. Comput. Chem.* **94** (2025) 135–155.

[39] X. Wang, Y. Jiang, H. Liu, H. Yuan, D. Huang, T. Wang, Research progress of multi-enzyme complexes based on the design of scaffold protein, *Bioresour. Bioprocess.* **10** (2023) #72.

[40] J. Yang, Y. Zhang, T. Yildirim, J. Zhang, A model predictive control algorithm based on biological regulatory mechanism and operational research, *IEEE/CAA J. Autom. Sin.* **10** (2023) 2174–2176.

[41] E. Zeidler, *Nonlinear Functional Analysis and Its Applications: II/B: Nonlinear Monotone Operators*, Springer, New York, 2013.